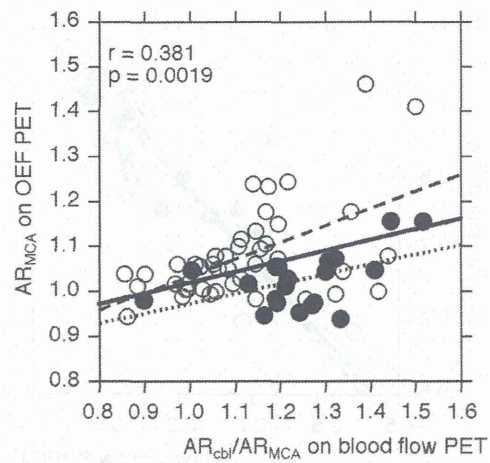


**Fig. 2** Correlation between  $AR_{cbl}$  (asymmetry ratio in the cerebellar hemispheric ROI) on blood flow PET and  $AR_{MCA}$  (asymmetry ratio in the MCA ROI) on blood flow PET (**a**) or  $AR_{MCA}$  on  $CMRO_2$  PET (**b**) in patients. In **b**, open and closed circles denote patients undergoing early and late PET studies, respectively; solid line ( $Y=0.399X+0.503$ ), dashed line ( $Y=0.783X+0.177$ ), and dotted line ( $Y=0.346X+0.492$ ) denote the regression lines of all patients, those undergoing early PET study and those undergoing late PET study, respectively

early and late PET studies, their intercepts were significantly lower in an equation of patients undergoing late PET study than in an equation of patients undergoing early PET study ( $p=0.0001$ , mean difference 0.096, 95 % CI 0.051–0.140) (Fig. 4c). The correlation coefficient was higher when reanalyzed in the 43 patients undergoing early PET study ( $r=0.653$ , 95 % CI 0.439–0.797,  $p<0.0001$ ).

$AR_{cbl}/AR_{MCA}$  on blood flow SPECT correlated with  $AR_{MCA}$  on OEF PET ( $r=0.459$ , 95 % CI 0.239–0.635,  $p=0.0001$ ) in patients; while the slopes of the regression lines between these two were statistically similar among equations of patients undergoing early and late PET studies, their intercepts were significantly lower in an equation of

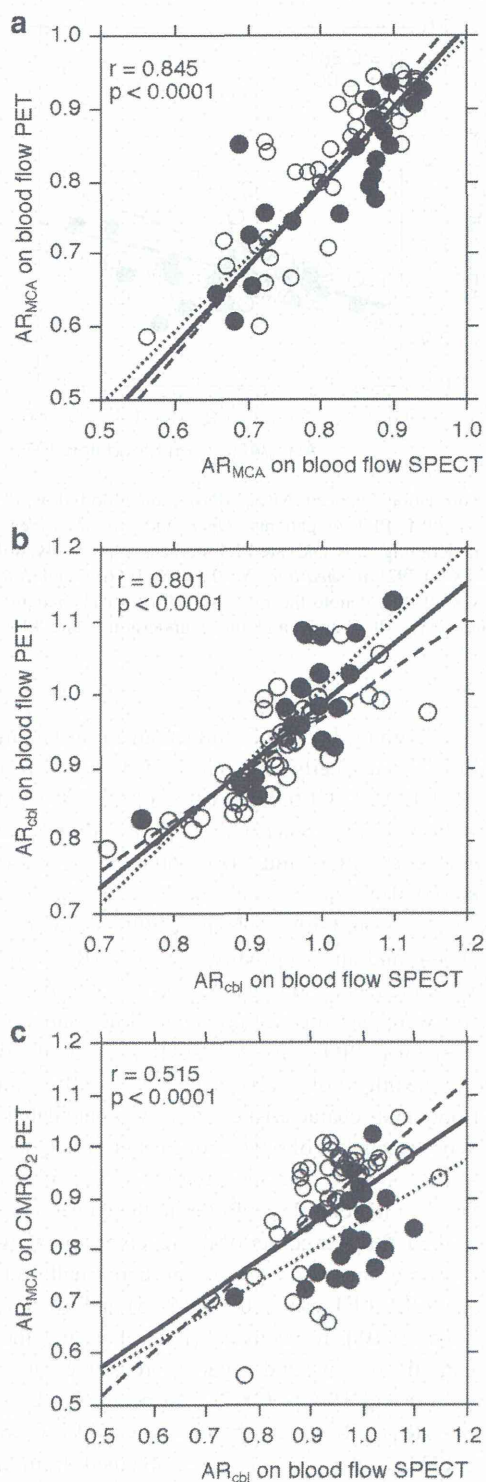


**Fig. 3** Correlation between  $AR_{cbl}/AR_{MCA}$  on blood flow PET and  $AR_{MCA}$  on OEF PET in patients. Open and closed circles denote patients undergoing early and late PET studies, respectively; solid line ( $Y=0.234X+0.792$ ), dashed line ( $Y=0.374X+0.661$ ), and dotted line ( $Y=0.216X+0.757$ ) denote the regression lines of all patients, those undergoing early PET study and those undergoing late PET study, respectively

patients undergoing late PET study than in an equation of patients undergoing early PET study ( $p=0.0032$ , mean difference 0.094, 95 % CI 0.0328–0.155) (Fig. 5). The correlation coefficient was higher when reanalyzed in 43 patients undergoing early PET study ( $r=0.609$ , 95 % CI 0.363–0.762,  $p<0.0001$ ).

The  $AR_{MCA}$  on OEF PET in healthy volunteers was  $1.001\pm0.044$ , and an abnormally elevated  $AR_{MCA}$  on OEF PET was defined as a value greater than 1.089. As a result, 15 patients were classified as having an abnormally elevated  $AR_{MCA}$  on OEF PET. The  $AR_{cbl}/AR_{MCA}$  on blood flow SPECT in healthy volunteers was  $0.999\pm0.051$ , and the receiver-operating characteristic curve was calculated in increments or decrements of 0.974 from 1.484 in  $AR_{cbl}/AR_{MCA}$  on blood flow SPECT. The sensitivity and specificity for the  $AR_{cbl}/AR_{MCA}$  on blood flow SPECT in the cutoff point lying closest to the left upper corner of the receiver-operating characteristic curve for detection of an abnormally elevated  $AR_{MCA}$  on OEF PET was 100 % (15/15) and 58 % (28/48) (cutoff point 1.101), respectively (Fig. 5). Using the same cutoff point, the positive and negative predictive values were 43 % (15/35) and 100 % (28/28), respectively. The cutoff point for  $AR_{cbl}/AR_{MCA}$  on blood flow SPECT was the mean+2 SDs of the control value obtained from normal subjects.

When reanalyzed in 43 patients undergoing early PET study using the same cutoff point, the sensitivity, specificity, and positive and negative predictive values for the  $AR_{cbl}/AR_{MCA}$  on blood flow SPECT for detection of an abnormally elevated  $AR_{MCA}$  on OEF PET were 100 % (13/13), 83 % (25/30), 72 % (13/18) and 100 % (25/25), respectively (Fig. 5).



Representative PET and SPECT images in two patients with unilateral ICA occlusion and reduced blood flow in the affected cerebral hemisphere on blood flow SPECT imaging are shown in Fig. 6 (patient with an abnormally elevated

**Fig. 4** Correlation between  $AR_{MCA}$  on blood flow SPECT and  $AR_{MCA}$  on blood flow PET in patients (a). Correlation between  $AR_{cbl}$  on blood flow SPECT and  $AR_{cbl}$  on blood flow PET in patients (b). Correlation between  $AR_{cbl}$  on blood flow SPECT and  $AR_{MCA}$  on  $CMRO_2$  PET in patients (c). *Open and closed circles* denote patients undergoing early and late PET studies, respectively; *solid lines* ( $Y=1.106X-0.087$  for a,  $Y=0.834X+0.151$  for b, and  $Y=0.682X+0.232$  for c), *dashed lines* ( $Y=1.163X+0.360$  for a,  $Y=0.690X+0.275$  for b, and  $Y=0.866X+0.090$  for c), and *dotted lines* ( $Y=1.008X-0.012$  for a,  $Y=0.962X+0.048$  for b, and  $Y=0.591X+0.259$  for c) denote the regression lines of all patients, those undergoing early PET study and those undergoing late PET study, respectively

$AR_{MCA}$  on OEF PET) and Fig. 7 (patient without an abnormally elevated  $AR_{MCA}$  on OEF PET).

## Discussion

The present study demonstrated that the ratio of contralateral-to-affected side blood flow asymmetry in the cerebellar hemisphere to affected-to-contralateral side blood flow asymmetry in the cerebral hemisphere on PET and SPECT correlates with affected-to-contralateral side OEF asymmetry in the cerebral hemisphere on PET in patients with chronic unilateral MCA or ICA occlusive disease.

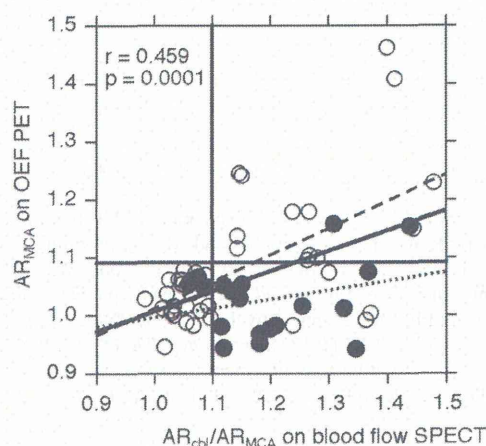


**Fig. 5** Correlation between  $AR_{cbl}/AR_{MCA}$  on blood flow SPECT and  $AR_{MCA}$  on OEF PET in patients. The plot of the relationship between these two values reveals four groups of results: *right upper* those with elevated  $AR_{cbl}/AR_{MCA}$  on blood flow SPECT and elevated  $AR_{MCA}$  on OEF PET (true-positive); *left upper* those with only elevated  $AR_{MCA}$  on OEF PET (false-negative); *left lower* those without elevated  $AR_{cbl}/AR_{MCA}$  on blood flow SPECT and without elevated  $AR_{MCA}$  on OEF PET (true-negative); and *right lower* those with only elevated  $AR_{cbl}/AR_{MCA}$  on blood flow SPECT (false-positive). *Vertical and horizontal lines* denote mean +2 SDs for  $AR_{cbl}/AR_{MCA}$  on blood flow SPECT and mean +2 SDs for  $AR_{MCA}$  on OEF PET obtained in healthy volunteers, respectively. *Open and closed circles* denote patients undergoing early and late PET studies, respectively; *solid line* ( $Y=0.345X+0.661$ ), *dashed line* ( $Y=0.467X+0.546$ ), and *dotted line* ( $Y=0.157X+0.837$ ) denote the regression lines of all patients, those undergoing early PET study and those undergoing late PET study, respectively



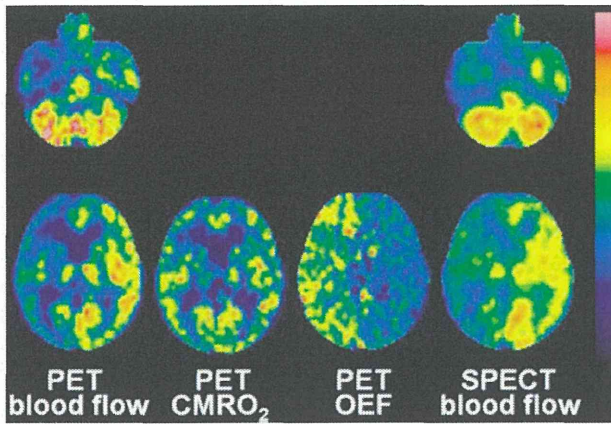


**Fig. 6** A 52-year-old man with symptomatic occlusion of the right ICA. The degree of blood flow asymmetry on PET is considerably greater in the MCA territory than in the cerebellar hemisphere.  $CMRO_2$  asymmetry in the MCA territory is not observed and OEF asymmetry in the MCA territory is evident on PET. While blood flow asymmetry in the MCA territory is evident on SPECT, blood flow asymmetry in the cerebellar hemisphere is not observed on SPECT

Further, this blood flow ratio on SPECT detects misery perfusion in the affected cerebral hemisphere in such patients.

When a patient with a unilateral chronic ICA or MCA occlusive disease exhibits an increase in OEF in the ipsilateral cerebral hemisphere, blood flow in that hemisphere is essentially reduced. On the other hand, even in patients with unilateral MCA occlusive disease, the blood flow and OEF values may be decreased and increased, respectively, in the territory of the contralateral MCA as well as in the territory of the ipsilateral MCA [26]. However, in such patients, blood flow and OEF was considerably lower and higher, respectively, in the affected MCA territory than in the

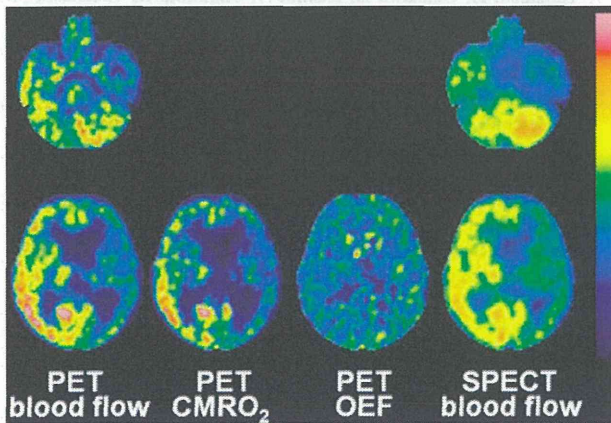


**Fig. 7** A 65-year-old man with symptomatic occlusion of the left MCA. Blood flow asymmetry on PET is evident in the cerebellar hemisphere as well as in the MCA territory.  $CMRO_2$  asymmetry in the MCA territory is also evident and OEF asymmetry in the MCA territory is not observed on PET. Blood flow asymmetry on SPECT is evident in the cerebellar hemisphere as well as in the MCA territory

contralateral MCA territory, and the  $AR_{MCA}$  on brain perfusion SPECT with  $^{123}I$ -IMP was less than 0.933 [10]. Thus, only patients with this condition on brain perfusion SPECT with  $^{123}I$ -IMP finally entered into the present study.

Although the degree of blood flow asymmetry in the MCA and cerebellar hemispheric ROIs strongly correlated when comparing assessments by SPECT and PET, the degree of blood flow asymmetry was underestimated on SPECT when compared with PET in half of our patients. These findings were also illustrated in blood flow asymmetry in the cerebellar hemispheres (Fig. 6). While a previous study demonstrated a strong correlation between CBF as assessed by  $^{123}I$ -IMP SPECT and CBF as assessed by PET, the former value tended to be underestimated as CBF increased [20]. This may be mainly due to the limited first-pass extraction fraction of  $^{123}I$ -IMP in the brain [20].

Yamauchi et al. measured brain blood flow and metabolism using PET in patients with unilateral ICA or MCA occlusive disorders and showed that while the degree of blood flow asymmetry in the MCA territory did not differ between patients with and without CCH, the degree of  $CMRO_2$  asymmetry in the MCA territory was significantly greater in patients with CCH and correlated with the degree of CCH [19]. Results from our PET studies were consistent with these previous findings and further demonstrated that the degree of CCH underestimated the degree of  $CMRO_2$  asymmetry in the MCA territory in patients when assessed at later than 3 months after the last ischemic event. Several studies reported that CCH was not always seen in patients with decreased  $CMRO_2$  in the cerebral hemisphere ipsilateral to a major cerebral artery occlusion [27] and often disappeared 2–3 months after onset in patients with hypertensive putaminal hemorrhage [28]. The present results support these findings and suggest that while CCH essentially reflects  $CMRO_2$  asymmetry in the cerebral hemisphere, this phenomenon may resolve over a few months after the last supratentorial cerebrovascular event despite the presence of the  $CMRO_2$  asymmetry.

Several investigators have suggested that patients with reduced CBF in the cerebral hemisphere ipsilateral to a major cerebral artery occlusive disease might have increased OEF in the hemisphere when CCH was not evident on PET [2, 19, 29]. This notion is supported by results from the present study in which the ratio of the degree of CCH to the degree of blood flow asymmetry in the MCA territory correlated with OEF asymmetry in the MCA territory. However, this blood flow ratio overestimated the OEF asymmetry in patients who were assessed at later than 3 months after the last ischemic event, which is related to the fact that CCH resolved over 3 months after the last cerebrovascular event despite the presence of  $CMRO_2$  asymmetry in the cerebral hemisphere.

Comparison of the present SPECT and PET studies demonstrated that the degree of CCH on SPECT correlated with



the degree of CMRO<sub>2</sub> asymmetry in the MCA territory on PET and that the ratio of the degree of CCH to the degree of blood flow asymmetry in the MCA territory on SPECT reflected OEF asymmetry in the MCA territory. Further, this blood flow ratio on SPECT detected misery perfusion in the affected cerebral hemisphere with a sensitivity and negative predictive value of 100 %. Although the specificity and positive predictive value were relatively low due to CCH resolving over 3 months after the last cerebrovascular event despite the presence of CMRO<sub>2</sub> asymmetry in the cerebral hemisphere, the simplicity of requiring only the evaluation of asymmetry on blood flow images makes the present SPECT method practical. The present SPECT method also has the advantage of not requiring acetazolamide, which is otherwise associated with a significant risk of various adverse side effects [13, 14]. In particular, this SPECT method is useful as a screening test to determine whether a PET study is needed in patients within 3 months after the last ischemic event.

The present study possesses limitations that require discussion. First, in patients with subcortical infarctions, in addition to primary ischemic cortical damage, secondary cerebral cortical hypometabolism due to a transneuronal mechanism and cerebrotocerebellar tract damage are responsible for CCH [19]. In particular, deep infarcts destroying most of the internal capsule frequently cause severe CCH [18]. Even an infarction limited to the posterior limb of the internal capsule causes CCH without hypometabolism in the ipsilateral cerebral cortex [30], resulting in CCH without regard to cerebral cortical metabolic status in patients with unilateral ICA or MCA steno-occlusive disorders [19]. Patients with subcortical infarctions involving the posterior limb of the internal capsule were thus excluded from the present study. Second, normal values were obtained from healthy subjects who were younger than the patients who enrolled in this study. Abnormally elevated AR<sub>MCA</sub> on OEF PET was defined as a value greater than the mean+2 SDs (1.089) of the normal values. Grubb et al. categorized patients with AR<sub>MCA</sub> on OEF PET of greater than 1.082 due to unilateral ICA steno-occlusive disease as having misery perfusion and reported that such patients are at high risk for subsequent stroke when treated medically [4]. Although the cutoff point for the AR<sub>MCA</sub> on OEF PET in the present study was approximately identical to that defined by Grubb et al., whether or not the AR<sub>cbi</sub>/AR<sub>MCA</sub> on blood flow SPECT can predict a higher risk of stroke recurrence remains unknown.

## Conclusion

The ratio of contralateral-to-affected side blood flow asymmetry in the cerebellar hemisphere to affected-to-contralateral side blood flow asymmetry in the cerebral hemisphere on PET and SPECT correlates with affected-to-contralateral side OEF

asymmetry in the cerebral hemisphere on PET in patients with chronic unilateral MCA or ICA occlusive disease. Further, this blood flow ratio on brain perfusion SPECT, which can be obtained using a single brain blood flow imaging study without acetazolamide challenge, detects misery perfusion in the affected cerebral hemisphere in such patients.

**Conflicts of interest** None.

**Open Access** This article is distributed under the terms of the Creative Commons Attribution License which permits any use, distribution, and reproduction in any medium, provided the original author(s) and the source are credited.

## References

1. Baron JC, Bousser MG, Rey A, Guillard A, Comar D, Castaigne P. Reversal of focal "misery-perfusion syndrome" by extra-intracranial arterial bypass in hemodynamic cerebral ischemia. A case study with 150 positron emission tomography. *Stroke* 1981;12:454–9.
2. Powers WJ. Cerebral hemodynamics in ischemic cerebrovascular disease. *Ann Neurol* 1991;29:231–40.
3. Yamauchi H, Fukuyama H, Nagahama Y, Nabatame H, Ueno M, Nishizawa S, et al. Significance of increased oxygen extraction fraction in five-year prognosis of major cerebral arterial occlusive diseases. *J Nucl Med* 1999;40:1992–8.
4. Grubb Jr RL, Derdeyn CP, Fritsch SM, Carpenter DA, Yundt KD, Videon TO, et al. Importance of hemodynamic factors in the prognosis of symptomatic carotid occlusion. *JAMA* 1998;280:1055–60.
5. Yamauchi H, Higashi T, Kagawa S, Nishii R, Kudo T, Sugimoto K, et al. Is misery perfusion still a predictor of stroke in symptomatic major cerebral artery disease? *Brain* 2012;135:2515–26.
6. Imaizumi M, Kitagawa K, Hashikawa K, Oku N, Teratani T, Takasawa M, et al. Detection of misery perfusion with split-dose 123I-iodoamphetamine single-photon emission computed tomography in patients with carotid occlusive diseases. *Stroke* 2002;33:2217–23.
7. Yamauchi H, Okazawa H, Kishibe Y, Sugimoto K, Takahashi M. Oxygen extraction fraction and acetazolamide reactivity in symptomatic carotid artery disease. *J Neurol Neurosurg Psychiatry* 2004;75:33–7.
8. Kuroda S, Shiga T, Houkin K, Ishikawa T, Katoh C, Tamaki N, et al. Cerebral oxygen metabolism and neuronal integrity in patients with impaired vasoreactivity attributable to occlusive carotid artery disease. *Stroke* 2006;37:393–8.
9. Hokari M, Kuroda S, Shiga T, Nakayama N, Tamaki N, Iwasaki Y. Combination of a mean transit time measurement with an acetazolamide test increases predictive power to identify elevated oxygen extraction fraction in occlusive carotid artery diseases. *J Nucl Med* 2008;49:1922–7.
10. Kuroda H, Ogasawara K, Suzuki T, Chida K, Aso K, Kobayashi M, et al. Accuracy of central benzodiazepine receptor binding potential/cerebral blood flow SPECT imaging for detecting misery perfusion in patients with unilateral major cerebral artery occlusive diseases: comparison with cerebrovascular reactivity to acetazolamide and cerebral blood flow SPECT imaging. *Clin Nucl Med* 2012;37:235–40.
11. Kuroda S, Houkin K, Kamiyama H, Mitsumori K, Iwasaki Y, Abe H. Long-term prognosis of medically treated patients with internal carotid or middle cerebral artery occlusion: can acetazolamide test predict it? *Stroke* 2001;32:2110–6.

12. Ogasawara K, Ogawa A, Yoshimoto T. Cerebrovascular reactivity to acetazolamide and outcome in patients with symptomatic internal carotid or middle cerebral artery occlusion: a xenon-133 single-photon emission computed tomography study. *Stroke* 2002;33:1857–62.
13. Ogasawara K, Tomitsuka N, Kobayashi M, Komoribayashi N, Fukuda T, Saitoh H, et al. Stevens-Johnson syndrome associated with intravenous acetazolamide administration for evaluation of cerebrovascular reactivity. Case report. *Neurol Med Chir (Tokyo)* 2006;46:161–3.
14. Saito H, Ogasawara K, Suzuki T, Kuroda H, Kobayashi M, Yoshida K, et al. Adverse effects of intravenous acetazolamide administration for evaluation of cerebrovascular reactivity using brain perfusion single-photon emission computed tomography in patients with major cerebral artery steno-occlusive diseases. *Neurol Med Chir (Tokyo)* 2011;51:479–83.
15. Komaba Y, Mishina M, Utsumi K, Katayama Y, Kobayashi S, Mori O. Crossed cerebellar diaschisis in patients with cortical infarction: logistic regression analysis to control for confounding effects. *Stroke* 2004;35:472–6.
16. Takasawa M, Watanabe M, Yamamoto S, Hoshi T, Sasaki T, Hashikawa K, et al. Prognostic value of subacute crossed cerebellar diaschisis: single-photon emission CT study in patients with middle cerebral artery territory infarct. *AJNR Am J Neuroradiol* 2002;23:189–93.
17. Baron JC, Boussier MG, Comar D, Soussaline F, Castaigne P. “Crossed cerebellar diaschisis”: a remote functional suppression secondary to supratentorial infarction in man. *J Cereb Blood Flow Metab* 1981;1:s500.
18. Pantano P, Baron JC, Samson Y, Boussier MG, Derouesne C, Comar D. Crossed cerebellar diaschisis: further studies. *Brain* 1986;109:677–94.
19. Yamauchi H, Fukuyama H, Yamaguchi S, Doi T, Ogawa M, Ouchi Y, et al. Crossed cerebellar hypoperfusion in unilateral major cerebral artery occlusive disorders. *J Nucl Med* 1992;33:1637–41.
20. Ogasawara K, Ito H, Sasoh M, Okuguchi T, Kobayashi M, Yukawa H, et al. Quantitative measurement of regional cerebrovascular reactivity to acetazolamide using 123I-N-isopropyl-p-iodoamphetamine autoradiography with SPECT: validation study using H2 15O with PET. *J Nucl Med* 2003;44:520–5.
21. Ibaraki M, Miura S, Shimosegawa E, Sugawara S, Mizuta T, Ishikawa A, et al. Quantification of cerebral blood flow and oxygen metabolism with 3-dimensional PET and 15O: validation by comparison with 2-dimensional PET. *J Nucl Med* 2008;49:50–9.
22. Frackowiak RS, Lenzi GL, Jones T, Heather JD. Quantitative measurement of regional cerebral blood flow and oxygen metabolism in man using 15O and positron emission tomography: theory, procedure, and normal values. *J Comput Assist Tomogr* 1980;4:727–36.
23. Lammertsma AA, Jones T. Correction for the presence of intravascular oxygen-15 in the steady-state technique for measuring regional oxygen extraction ratio in the brain: 1. Description of the method. *J Cereb Blood Flow Metab* 1983;3:416–24.
24. Nishimiya M, Matsuda H, Imabayashi E, Kuji I, Sato N. Comparison of SPM and NEUROSTAT in voxelwise statistical analysis of brain SPECT and MRI at the early stage of Alzheimer’s disease. *Ann Nucl Med* 2008;22:921–7.
25. Takeuchi R, Matsuda H, Yoshioka K, Yonekura Y. Cerebral blood flow SPET in transient global amnesia with automated ROI analysis by 3DSRT. *Eur J Nucl Med Mol Imaging* 2004;31:578–89.
26. Tanaka M, Shimosegawa E, Kajimoto K, Kimura Y, Kato H, Oku N, et al. Chronic middle cerebral artery occlusion: a hemodynamic and metabolic study with positron-emission tomography. *AJNR Am J Neuroradiol* 2008;29:1841–6.
27. Martin WR, Raichle ME. Cerebellar blood flow and metabolism in cerebral hemisphere infarction. *Ann Neurol* 1983;14:168–76.
28. Ishikawa Y, Mukawa J, Kinjo T, Mekaru S, Miyazato H, Takara E, et al. Crossed cerebellar diaschisis in putaminal hemorrhage—evaluation by the Xe-133 clearance method. *No To Shinkei* 1994;46:335–40.
29. Gibbs JM, Wise RJ, Leenders KL, Jones T. Evaluation of cerebral perfusion reserve in patients with carotid-artery occlusion. *Lancet* 1984;1:310–4.
30. Pappata S, Mazoyer B, Tran Dinh S, Cambon H, Levasseur M, Baron JC. Effects of capsular or thalamic stroke on metabolism in the cortex and cerebellum: a positron tomography study. *Stroke* 1990;21:519–24.

# Combined Measurement of Cerebral and Cerebellar Blood Flow on Preoperative Brain Perfusion SPECT Imaging Predicts Development of New Cerebral Ischemic Events After Endarterectomy for Symptomatic Unilateral Cervical Carotid Stenosis

Kohki Oikawa, MD, Kuniaki Ogasawara, MD, Hideo Saito, MD, Koji Yoshida, MD, Hiroaki Saura, MD, Yuiko Sato, MD, Kazunori Terasaki, PhD, Tsukasa Wada, MD, and Yoshitaka Kubo, MD

**Purpose:** The aim of this study was to determine whether the ratio of blood flow contralateral-to-affected asymmetry in the cerebellar hemisphere to blood flow affected-to-contralateral asymmetry in the middle cerebral artery (MCA) territory ( $AR_{cb}/AR_{MCA}$ ) on preoperative brain perfusion SPECT could identify patients at risk for new cerebral ischemic events after carotid endarterectomy (CEA) for symptomatic unilateral cervical carotid stenosis. For the purposes of this study, new cerebral ischemic events included neurological deficits and cerebral ischemic lesions on diffusion-weighted MRI.

**Methods:** Brain blood flow was assessed using  $^{123}I$ -IMP SPECT in 101 patients. A region of interest was automatically placed in the bilateral MCA territories and in the bilateral cerebellar hemispheres using a 3-dimensional stereotaxic region-of-interest template, and the  $AR_{cb}/AR_{MCA}$  was calculated. Diffusion-weighted MRI was performed within 3 days before and 24 hours after surgery. Patients were neurologically tested before induction of general anesthesia and after recovery from general anesthesia.

**Results:** New cerebral ischemic events after CEA were observed in 12 patients (12%). Multivariate analysis revealed that only high  $AR_{cb}/AR_{MCA}$  was significantly associated with the development of new postoperative cerebral ischemic events (95% confidence interval, 1.945–8.452;  $P = 0.0070$ ). The  $AR_{cb}/AR_{MCA}$  provided 75% sensitivity, 84% specificity, and 39% positive and 96% negative predictive values in predicting development of new postoperative cerebral ischemic events.

**Conclusions:** The  $AR_{cb}/AR_{MCA}$  on preoperative brain perfusion SPECT could identify patients at risk for new cerebral ischemic events after CEA for unilateral cervical carotid stenosis.

**Key Words:** carotid endarterectomy, cerebral ischemic event, brain perfusion, crossed cerebellar hypoperfusion, SPECT

(*Clin Nucl Med* 2013;38: 957–961)

Neurological deficits after carotid endarterectomy (CEA) are uncommon, occurring in up to 5% of patients.<sup>1–3</sup> Hemodynamic cerebral ischemia due to hemispheric hypoperfusion during internal carotid artery (ICA) clamping and the generation of emboli from the surgical site play significant roles in the development of new cerebral ischemic events, including new neurological deficits and new cerebral ischemic lesions on diffusion-weighted MRI (DWI) after CEA.<sup>4–11</sup>

Risk factors for the development of cerebral ischemic complications associated with CEA include preoperative impairments in cerebral hemodynamics.<sup>12,13</sup> Several investigators have demonstrated that a decrease in cerebrovascular reactivity to acetazolamide, as measured using SPECT, predicts the development of new postoperative cerebral ischemic events due to hemispheric hypoperfusion during ICA clamping<sup>12</sup> or emboli from the surgical site.<sup>13</sup> However, acetazolamide is associated with frequent and various adverse effects, including headache, nausea, dizziness, tinnitus, numbness of the extremities, and Stevens-Johnson syndrome.<sup>14,15</sup> In fact, 1 study demonstrated that 63% of patients who underwent SPECT study with acetazolamide challenge developed adverse effects after administration of acetazolamide, and these symptoms frequently impacted patients' activities of daily living, including the ability to engage in their jobs.<sup>15</sup> Thus, it would be beneficial to develop a different SPECT method of predicting the development of new cerebral ischemic events associated with CEA that does not require administration of acetazolamide.

Crossed cerebellar hypoperfusion (CCH) is defined as a reduction in blood flow in the cerebellar hemisphere contralateral to a supratentorial lesion.<sup>16</sup> This phenomenon can be demonstrated on brain perfusion images obtained by SPECT or by PET.<sup>16–19</sup> The mechanism underlying CCH reportedly consists of disruption of the corticopontocerebellar pathway that causes functional deafferentation and transneuronal metabolic depression of the contralateral cerebellar hemisphere.<sup>18,19</sup> In patients with unilateral carotid artery occlusive disease, contralateral-to-affected side blood flow asymmetry in the cerebellar hemisphere reflects cerebral metabolic rate of oxygen ( $CMRO_2$ ) in the affected cerebral hemisphere relative to that in the contralateral cerebral hemisphere.<sup>20</sup> Oxygen extraction fraction (OEF), one of the key parameters of cerebral hemodynamics,<sup>21,22</sup> is a function of  $CMRO_2/CBF$ , and a recent study has demonstrated that the ratio of blood flow asymmetry in the cerebellar hemisphere to blood flow asymmetry in the cerebral hemisphere on brain perfusion SPECT correlates with PET-OEF asymmetry in the cerebral hemisphere. Furthermore, this blood flow ratio detects misery perfusion in the affected cerebral hemisphere in patients with unilateral occlusion of the middle cerebral artery (MCA) or ICA.<sup>23</sup>

The aim of the present study was to determine whether the ratio of blood flow asymmetry in the cerebellar hemisphere to blood flow asymmetry in the cerebral hemisphere on preoperative brain perfusion SPECT could identify patients at risk for new cerebral ischemic events after CEA for symptomatic unilateral cervical carotid stenosis.

## METHODS

### Patients

A total of 101 patients (94 men and 7 women), aged 51 to 85 years (mean, 70 years), with symptomatic unilateral ICA stenosis

Received for publication June 11, 2013; revision accepted September 3, 2013.

From the Department of Neurosurgery and Cyclotron Research Center, Iwate Medical University, Morioka, Japan.

Conflicts of interest and sources of funding: none declared.

Reprints: Kuniaki Ogasawara, MD, Department of Neurosurgery, Iwate Medical University, 19-1 Uchimaru, Morioka, 020-8505 Japan.

E-mail: kuogasa@iwate-med.ac.jp.

Copyright © 2013 by Lippincott Williams & Wilkins

ISSN: 0363-9762/13/3812–0957

( $\geq 70\%$ ) and useful residual function (modified Rankin disability scale 0, 1, or 2) who underwent CEA between 2 weeks and 3 months after the last ischemic event were enrolled in the present study. None of these patients experienced clinical symptoms suggesting ischemic episodes in the vertebrobasilar territory. Concomitant disease states and symptoms were recorded, including 92 patients with hypertension, 40 patients with diabetes mellitus, and 52 patients with dyslipidemia.

All patients underwent preoperative angiography with arterial catheterization. The overall average degree of ICA stenosis was  $87.2\% \pm 8.5\%$ , with a range of 70% to 99%, as per the North American Symptomatic Carotid Endarterectomy Trial.<sup>3</sup> No patient had occlusion or stenosis of greater than 50% in the contralateral ICA, MCA, and vertebrobasilar arteries. All patients also underwent preoperative T1- and T2-weighted imaging and DWI, and no patients had infarcts involving the posterior limb of the internal capsule in the affected cerebral hemisphere and gross morphological alterations in the cerebellum and brain stem.

This protocol was reviewed and approved by our institutional ethics committee, and written informed consent was obtained from all patients or their next of kin.

### Brain Perfusion SPECT Study

SPECT studies were performed using a ring-type SPECT scanner, a Headtome-SET080 (Shimadzu Corp, Kyoto, Japan), which provides 31 tomographic images simultaneously.<sup>24</sup> The spatial resolution of the scanner with a low-energy, all-purpose collimator was 13-mm full width at half maximum at the center of the FOV, and the slice thickness was 25-mm full width at half maximum at the FOV center. Image slices were taken at 5-mm center-to-center spacing parallel to the orbitomeatal line. The images were reconstructed using the weighted-filtered backprojection technique, in which the attenuation correction was made by detecting the edge of the object. An attenuation coefficient of  $0.065 \text{ cm}^{-1}$ , a Butterworth filter (cutoff = 0.45 cycle/cm; order = 3), and a ramp filter were used for image reconstruction.

The distribution of brain perfusion was assessed using  $^{123}\text{I}$ -IMP and SPECT within 7 days before CEA. The  $^{123}\text{I}$ -IMP SPECT study was performed as described previously.<sup>24</sup> Briefly, after a 1-minute intravenous infusion of 222 MBq of  $^{123}\text{I}$ -IMP (5-mL volume) at a constant rate of 5 mL/min and a 1-minute infusion of physiologic saline at the same rate, data acquisition was performed at a midscan time of 30 minutes for a scan duration of 20 minutes.

All SPECT images were transformed into the standard brain size and shape by linear and nonlinear transformation using SPM2 for anatomic standardization.<sup>25</sup> Thus, brain images from all subjects had the same anatomic format. Three hundred eighteen constant regions of interest (ROIs) were automatically placed in both the cerebral and cerebellar hemispheres using a 3-dimensional stereotaxic ROI template with SPM2 (FUJIFILM RI Pharma Co, Ltd, Tokyo, Japan).<sup>26</sup> The ROIs were grouped into 10 segments (callosomarginal, pericallosal, precentral, central, parietal, angular, temporal, posterior, hippocampus, and cerebellar) in each hemisphere according to the arterial supply. Five (precentral, central, parietal, angular, and temporal) of these 10 segments were combined and defined as an ROI perfused by the MCA (Fig. 1). The mean value of radioactive counts on  $^{123}\text{I}$ -IMP SPECT images was measured in the bilateral MCAs and in cerebellar hemispheric ROIs. Then, the asymmetry ratio in the MCA ROI ( $AR_{MCA}$ ) was calculated as the value in the cerebral hemisphere ipsilateral to the side of the stenosed ICA divided by the value in the contralateral cerebral hemisphere. The asymmetry ratio in the cerebellar hemispheric ROI ( $AR_{cbi}$ ) was calculated as the value in the cerebellar hemisphere contralateral to the side of the stenosed ICA divided by the value in the ipsilateral

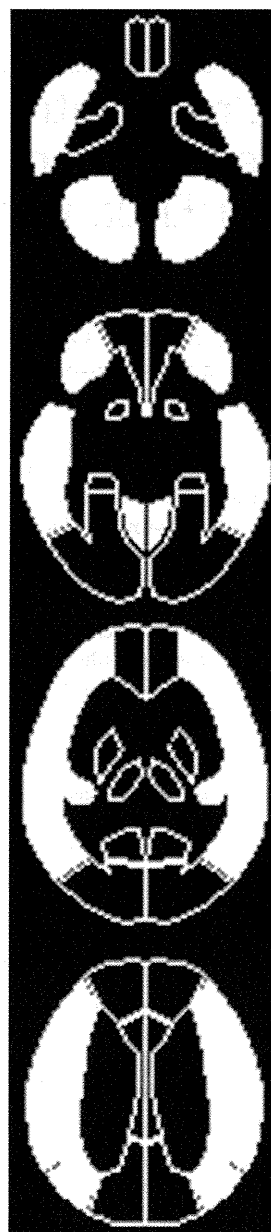


**FIGURE 1.** Diagrams showing the ROIs of a 3-dimensional stereotaxic ROI template on brain SPECT. The white ROIs indicate the bilateral cerebellar hemispheres and cortical territories perfused by the bilateral MCAs.

cerebellar hemisphere. Finally, the value of  $AR_{cbi}$  divided by  $AR_{MCA}$  ( $AR_{cbi}/AR_{MCA}$ ) was calculated for each patient.

Using the same method, 10 normal male subjects (aged 35–52 years; mean age, 43 years) were studied to obtain control values.<sup>23</sup> The control value of  $AR_{cbi}/AR_{MCA}$  was  $0.999 \pm 0.051$  when the left cerebral hemisphere was defined as the affected side.<sup>23</sup>

### Diffusion-Weighted MRI

Diffusion-weighted MRI was performed using a 1.5-T whole-body imaging system (Signa MR/I; GE Healthcare, Milwaukee, Wis) within 3 days before and 24 hours after surgery. The images were acquired using a single-shot spin-echo echo-planar imaging. A neuroradiologist who was blinded to the patients' clinical information



**TABLE 1.** Risk Factors for the Development of new Postoperative Cerebral Ischemic Events

Risk Factors	New Postoperative Cerebral Ischemic Events		P
	Yes (n = 12)	No (n = 89)	
Age, mean ± SD, y	70.0 ± 7.1	69.7 ± 7.2	0.8213
Male, n (%)	12 (100)	82 (92)	0.5946
Hypertension, n (%)	12 (100)	80 (90)	0.5942
Diabetes mellitus, n (%)	6 (50)	34 (38)	0.5334
Dyslipidemia, n (%)	6 (50)	46 (52)	>0.9999
Degree of ICA stenosis, mean ± SD, %	91.2 ± 7.3	86.7 ± 8.5	0.0490
Duration of ICA clamping, mean ± SD, min	36.3 ± 6.7	36.0 ± 5.3	0.9121
Preoperative AR <sub>cbi</sub> /AR <sub>MCA</sub>	1.220 ± 0.171	1.076 ± 0.117	0.0014

AR<sub>cbi</sub> indicates asymmetry ratio in cerebellar hemispheric ROI; AR<sub>MCA</sub>, asymmetry ratio in MCA ROI.

was employed to analyze the images and identify the development of new postoperative ischemic lesions.

**Assessment of Neurological Deficits**

All patients were neurologically tested immediately before induction of general anesthesia and after recovery from general anesthesia by a neurologist who was blinded to the patients’ clinical information. The presence or absence of new postoperative neurological deficits was recorded.

**Intraoperative and Postoperative Management**

All patients received antiplatelet therapy until the morning of the day on which CEA was performed. Furthermore, all patients underwent surgery under general anesthesia. Blood pressure was kept stable in a range ±20% of the preoperative level throughout the procedure by adjusting the depth of anesthesia or, if needed, by intravenous administration of a vasodilator (nitroglycerin) or a vasoconstrictor (theoadrenalin). An intraluminal shunt was not used in these procedures. The mean duration of ICA clamping was 36 minutes, ranging from 22 to 49 minutes.

**Statistical Analysis**

Data are expressed as the mean ± SD. The relationship between parameters in patients and those in control subjects was evaluated using the Mann-Whitney U test. The relationship between each variable and the development of new postoperative cerebral ischemic events (neurological deficits and/or cerebral ischemic lesions on DWI) was evaluated with univariate analysis using the Mann-Whitney U test or χ<sup>2</sup> test. A multivariate statistical analysis of factors related to development of new postoperative cerebral ischemic events was also performed using a logistic regression model. Variables with P < 0.2 in the univariate analyses were selected for analysis in the final model. Differences were deemed statistically significant if P < 0.05. The accuracy of AR<sub>cbi</sub>/AR<sub>MCA</sub> to predict the development of new postoperative cerebral ischemic events was determined by a receiver operating characteristic curve when the relationship between these 2 variables was significant. The curve was calculated in increments or decrements of 1 SD from the mean value of AR<sub>cbi</sub>/AR<sub>MCA</sub> obtained in control subjects.

**RESULTS**

Of the 101 patients studied, 9 patients (9%) developed new postoperative ischemic lesions on DWI in the cerebral hemisphere

ipsilateral to CEA. All the new ischemic lesions were spotty, and their diameters were 1.5 cm or less. Five patients (5%) developed new postoperative neurological deficits: 3 (3%) with new postoperative cerebral ischemic lesions on DWI and 2 (2%) without new postoperative cerebral ischemic lesions on DWI. Although those deficits resolved completely within 12 hours in 3 patients, the neurological deficits in the remaining 2 patients persisted for more than 24 hours after surgery. Thus, a total of 12 patients (12%) experienced new postoperative ischemic events (postoperative cerebral ischemic lesions on DWI and/or postoperative neurological deficits).

AR<sub>cbi</sub>/AR<sub>MCA</sub> in the 101 patients studied ranged from 0.865 to 1.675 (mean ± SD, 1.093 ± 0.132) and was significantly higher than that in control subjects (P < 0.0001).

Results of univariate analysis of factors related to the development of new postoperative ischemic events are summarized in Table 1. The degree of ICA stenosis and preoperative AR<sub>cbi</sub>/AR<sub>MCA</sub> were significantly higher in patients with new postoperative ischemic events than in those without new postoperative ischemic events. Other variables were not significantly associated with the development of new postoperative ischemic events. After eliminating closely related variables in the univariate analyses, the following confounders (P < 0.2) were adopted in the logistic regression model for the multivariate analysis: degree of ICA stenosis and preoperative AR<sub>cbi</sub>/AR<sub>MCA</sub>. Multivariate analysis revealed that high preoperative AR<sub>cbi</sub>/AR<sub>MCA</sub> was significantly associated with the development of new postoperative ischemic events (95% confidence interval, 1.945–8.452; P = 0.0070).

Sensitivity and specificity for the AR<sub>cbi</sub>/AR<sub>MCA</sub> in the cutoff point lying closest to the left upper corner of the receiver operating characteristic curve for prediction of the development of new postoperative ischemic events were 75% (9/12) and 84% (75/89) (cutoff point = 1.152; the mean + 3 SDs of the control value obtained from control subjects), respectively (Fig. 2). With the same cutoff point, the positive and negative predictive values were 39% (9/23) and 96% (75/78), respectively.

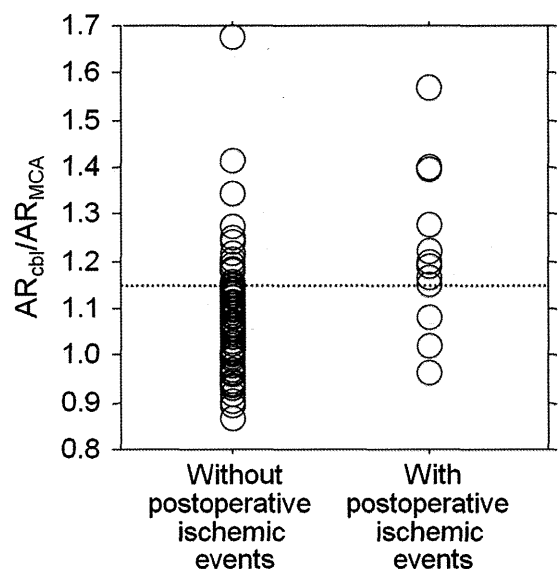


**FIGURE 2.** Relationship between the ratio of blood flow contralateral-to-affected asymmetry in the cerebellar hemisphere to blood flow affected-to-contralateral asymmetry in the MCA territory (AR<sub>cbi</sub>/AR<sub>MCA</sub>) and postoperative cerebral ischemic events. Dashed horizontal line denotes mean + 3 SDs of AR<sub>cbi</sub>/AR<sub>MCA</sub> obtained in healthy volunteers.



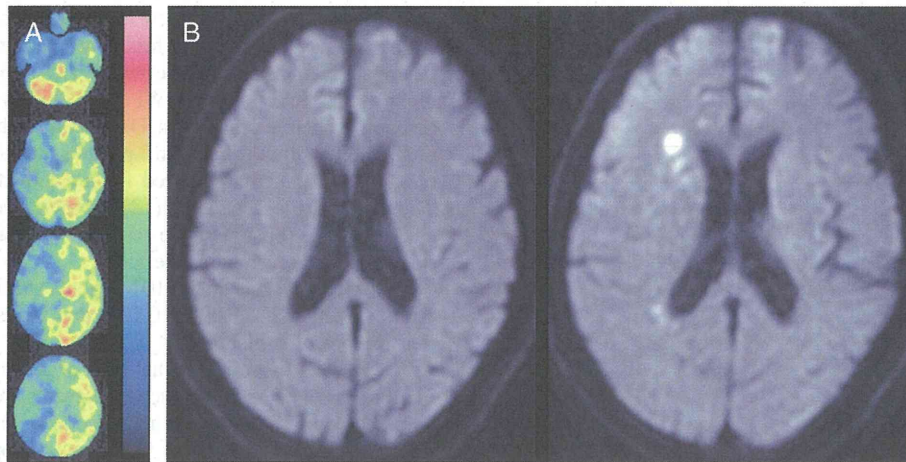


**FIGURE 3.** A 72-year-old man with symptomatic right ICA stenosis (95%) exhibiting left hemiparesis upon recovery from general anesthesia after CEA. Ten hours later, the hemiparesis resolved. **A**, While blood flow asymmetry is observed in the cerebellar hemisphere and in the MCA territory, the asymmetry is more prominent in the latter than in the former. **B**, Diffusion-weighted MRI before surgery shows no abnormal findings in the right cerebral hemisphere (left) in which new multiple high-intensity lesions develop after surgery (right).

SPECT and MR images for a patient who developed transient neurological deficits and cerebral ischemic lesions on DWI after surgery are illustrated in Figure 3.

## DISCUSSION

The present study demonstrated that the ratio of blood flow asymmetry in the cerebellar hemisphere to blood flow asymmetry in the cerebral hemisphere on preoperative brain perfusion SPECT could identify patients at risk for new cerebral ischemic events after CEA for unilateral cervical carotid stenosis.

Hemodynamic compromise due to chronic cerebral ischemia in ICA stenosis implies that collateral blood flow is not sufficient to maintain the cerebral blood flow against a further decrease in perfusion pressure. Because ICA clamping during CEA may cause a critical reduction of cerebral perfusion in the area with hemodynamic compromise, cerebral ischemic events may develop more frequently in patients with hemodynamic compromise than in those without. One study reported that the reduction of preoperative cerebrovascular reactivity to acetazolamide measured by brain perfusion SPECT correlates with a high risk of significant cerebral ischemia during ICA clamping.<sup>12</sup>

Microembolic signals on intraoperative transcranial Doppler monitoring of the MCA are detected in more than 90% of patients undergoing CEA.<sup>4,5</sup> In particular, there is a significant correlation between the number of microembolic signals during dissection of the carotid arteries and the development of new postoperative ischemic lesions on DWI.<sup>4-9</sup> According to the concept proposed by Caplan and Hennerici,<sup>27</sup> preexisting hemodynamic impairment may also facilitate the onset of ischemia due to emboli generated from a proximal lesion. One study demonstrated that the reduction of preoperative cerebrovascular reactivity to acetazolamide measured by brain perfusion SPECT predicts the development of new postoperative cerebral ischemic lesions on DWI that are caused by microemboli generated during carotid dissection in CEA.<sup>13</sup>

The present study demonstrated that high preoperative  $AR_{\text{cbI}}/AR_{\text{MCA}}$  was a significant independent predictor of new postoperative cerebral ischemic events. Because high  $AR_{\text{cbI}}/AR_{\text{MCA}}$  suggests the presence of “misery perfusion” in the affected hemisphere,<sup>23</sup> our findings support the theory that preoperative hemodynamic impairment

is associated with the development of cerebral ischemic events due to intraoperative emboli as well as due to significant hemispheric hypoperfusion during ICA clamping.

In the present study, while  $AR_{\text{cbI}}/AR_{\text{MCA}}$  provided low positive and high negative predictive values for the prediction of new postoperative cerebral ischemic events, both values were similar to those associated with cerebrovascular reactivity to acetazolamide on brain perfusion SPECT (28% positive predictive value, 96% negative predictive value).<sup>28</sup> Thus,  $AR_{\text{cbI}}/AR_{\text{MCA}}$  may be a useful and alternative SPECT method for the prediction of new postoperative cerebral ischemic events because of the simplicity of requiring only the evaluation of asymmetry on blood flow images. The present SPECT method also has the advantage of not requiring acetazolamide, which is otherwise associated with a significant risk of various adverse effects.<sup>14,15</sup>

The present study possesses limitations that require discussion. First, this study included only patients within 3 months after the last ischemic event. Although contralateral-to-affected side blood flow asymmetry in the cerebellar hemisphere essentially reflects  $CMRO_2$  in the affected cerebral hemisphere relative to that in the contralateral cerebral hemisphere,<sup>20,23</sup> the degree of the blood flow asymmetry in the cerebellar hemisphere underestimates the degree of  $CMRO_2$  asymmetry in the cerebral hemisphere when assessed at later than 3 months after the last ischemic event.<sup>23</sup> These findings are supported by previous reports in which CCH was not always seen in patients with decreased  $CMRO_2$  in the cerebral hemisphere ipsilateral to a major cerebral artery occlusion.<sup>29</sup> In fact, CCH often disappeared 2 to 3 months after onset in patients with stroke.<sup>30</sup> As a result, while the  $AR_{\text{cbI}}/AR_{\text{MCA}}$  overestimates the OEF asymmetry in patients who are assessed at later than 3 months after the last ischemic event, the specificity (83%) and positive predictive value (72%) of the  $AR_{\text{cbI}}/AR_{\text{MCA}}$  for detection of the misery perfusion are elevated when assessed in patients within 3 months after the last ischemic event.<sup>23</sup> Thus, the accuracy of the  $AR_{\text{cbI}}/AR_{\text{MCA}}$  for the prediction of new cerebral ischemic events after CEA may decrease in patients who are assessed at later than 3 months after the last ischemic event.

Second, the study population included only patients with unilateral ICA stenosis and used blood flow asymmetry on SPECT images to detect cerebral hemodynamic impairment in the affected cerebral hemisphere. The impairment in cerebral hemodynamics is

more severe in patients with bilateral ICA steno-occlusive disease than in those with unilateral ICA steno-occlusive disease,<sup>31</sup> and impairments in bilateral cerebral hemodynamics in patients with bilateral ICA steno-occlusive disease may not be detected by the present SPECT method. Lastly, in patients with subcortical infarctions, secondary cerebral cortical hypometabolism due to transneuronal mechanisms and cerebrotocerebellar tract damage are responsible for CCH.<sup>20</sup> In particular, deep infarcts that destroy most of the internal capsule frequently cause severe CCH.<sup>19</sup> Even an infarction limited to the posterior limb of the internal capsule causes CCH without hypometabolism in the ipsilateral cerebral cortex,<sup>32</sup> resulting in underestimation of  $AR_{cb}/AR_{MCA}$  for the detection of misery perfusion.<sup>23</sup> The present study population did not include patients with infarctions involving the posterior limb of the internal capsule.

### CONCLUSIONS

The present study demonstrated that the ratio of blood flow asymmetry in the cerebellar hemisphere to blood flow asymmetry in the cerebral hemisphere on preoperative brain perfusion SPECT could identify patients at risk for new cerebral ischemic events after CEA for unilateral cervical carotid stenosis.

### REFERENCES

1. European Carotid Surgery Trialists' Collaborative Group. MRC European Carotid Surgery Trial: interim results for symptomatic patients with severe (70–99%) or with mild (0–29%) carotid stenosis. *Lancet*. 1991;337:1235–1243.
2. Executive Committee for the Asymptomatic Carotid Atherosclerosis Study. Endarterectomy for asymptomatic carotid artery stenosis. *JAMA*. 1995;273:1421–1428.
3. North American Symptomatic Carotid Endarterectomy Trial Collaborators. Beneficial effect of carotid endarterectomy in symptomatic patients with high-grade carotid stenosis. *N Engl J Med*. 1991;325:445–453.
4. Wolf O, Heider P, Heinz M, et al. Microembolic signals detected by transcranial Doppler sonography during carotid endarterectomy and correlation with serial diffusion-weighted imaging. *Stroke*. 2004;35:e373–e375.
5. Ackerstaff RG, Moons KG, van de Vlasakker CJ, et al. Association of intraoperative transcranial Doppler monitoring variables with stroke from carotid endarterectomy. *Stroke*. 2000;31:1817–1823.
6. Gavrilescu T, Babikian VL, Cantelmo NL, et al. Cerebral microembolism during carotid endarterectomy. *Am J Surg*. 1995;170:159–164.
7. Verhoeven BA, de Vries JP, Pasterkamp G, et al. Carotid atherosclerotic plaque characteristics are associated with microembolization during carotid endarterectomy and procedural outcome. *Stroke*. 2005;36:1735–1740.
8. Gaunt ME, Martin PJ, Smith JL, et al. Clinical relevance of intraoperative embolization detected by transcranial Doppler ultrasonography during carotid endarterectomy: a prospective study of 100 patients. *Br J Surg*. 1994;81:1435–1439.
9. Jansen C, Ramos LM, van Heesewijk JP, et al. Impact of microembolism and hemodynamic changes in the brain during carotid endarterectomy. *Stroke*. 1994;25:992–997.
10. Mille T, Tachimiri ME, Klersy C, et al. Near infrared spectroscopy monitoring during carotid endarterectomy: which threshold value is critical? *Eur J Vasc Endovasc Surg*. 2004;27:646–650.
11. van der Schaaf IC, Horn J, Moll FL, et al. Transcranial Doppler monitoring after carotid endarterectomy. *Ann Vasc Surg*. 2005;19:19–24.
12. Kim JS, Moon DH, Kim GE, et al. Acetazolamide stress brain-perfusion SPECT predicts the need for carotid shunting during carotid endarterectomy. *J Nucl Med*. 2000;41:1836–1841.
13. Aso K, Ogasawara K, Sasaki M, et al. Preoperative cerebrovascular reactivity to acetazolamide measured by brain perfusion SPECT predicts development of cerebral ischemic lesions caused by microemboli during carotid endarterectomy. *Eur J Nucl Med Mol Imaging*. 2009;36:294–301.
14. Ogasawara K, Tomitsuka N, Kobayashi M, et al. Stevens-Johnson syndrome associated with intravenous acetazolamide administration for evaluation of cerebrovascular reactivity. Case report. *Neurol Med Chir (Tokyo)*. 2006;46:161–163.
15. Saito H, Ogasawara K, Suzuki T, et al. Adverse effects of intravenous acetazolamide administration for evaluation of cerebrovascular reactivity using brain perfusion single-photon emission computed tomography in patients with major cerebral artery steno-occlusive diseases. *Neurol Med Chir (Tokyo)*. 2011;51:479–483.
16. Komaba Y, Mishina M, Utsumi K, et al. Crossed cerebellar diaschisis in patients with cortical infarction: logistic regression analysis to control for confounding effects. *Stroke*. 2004;35:472–476.
17. Takasawa M, Watanabe M, Yamamoto S, et al. Prognostic value of subacute crossed cerebellar diaschisis: single-photon emission CT study in patients with middle cerebral artery territory infarct. *AJNR Am J Neuroradiol*. 2002;23:189–193.
18. Baron JC, Bousser MG, Comar D, et al. “Crossed cerebellar diaschisis”: a remote functional suppression secondary to supratentorial infarction in man. *J Cereb Blood Flow Metab*. 1981;1:s500.
19. Pantano P, Baron JC, Samson Y, et al. Crossed cerebellar diaschisis: further studies. *Brain*. 1986;109:677–694.
20. Yamauchi H, Fukuyama H, Yamaguchi S, et al. Crossed cerebellar hypoperfusion in unilateral major cerebral artery occlusive disorders. *J Nucl Med*. 1992;33:1637–1641.
21. Gibbs JM, Wise RJ, Leenders KL, et al. Evaluation of cerebral perfusion reserve in patients with carotid-artery occlusion. *Lancet*. 1984;1:310–314.
22. Powers WJ. Cerebral hemodynamics in ischemic cerebrovascular disease. *Ann Neurol*. 1991;29:231–240.
23. Matsumoto Y, Ogasawara K, Saito H, et al. Detection of misery perfusion in the cerebral hemisphere with chronic unilateral major cerebral artery steno-occlusive disease using crossed cerebellar hypoperfusion: comparison of brain SPECT and PET imaging. *Eur J Nucl Med Mol Imaging*. 2013;40:1573–1581.
24. Ogasawara K, Ito H, Sasoh M, et al. Quantitative measurement of regional cerebrovascular reactivity to acetazolamide using [<sup>125</sup>I]iodoamphetamine autoradiographic method with single photon emission computed tomography: validation study using [<sup>15</sup>O] H<sub>2</sub>O positron emission tomography. *J Nucl Med*. 2003;44:520–525.
25. Nishimiya M, Matsuda H, Imabayashi E, et al. Comparison of SPM and NEUROSTAT in voxelwise statistical analysis of brain SPECT and MRI at the early stage of Alzheimer's disease. *Ann Nucl Med*. 2008;22:921–927.
26. Takeuchi R, Matsuda H, Yoshioka K, et al. Cerebral blood flow SPET in transient global amnesia with automated ROI analysis by 3DSRT. *Eur J Nucl Med Mol Imaging*. 2004;31:578–589.
27. Caplan LR, Hennerici M. Impaired clearance of emboli (washout) is an important link between hypoperfusion, embolism, and ischemic stroke. *Arch Neurol*. 1998;55:1475–1482.
28. Sato Y, Ogasawara K, Kuroda H, et al. Preoperative central benzodiazepine receptor binding potential and cerebral blood flow images on SPECT predict development of new cerebral ischemic events and cerebral hyperperfusion after carotid endarterectomy. *J Nucl Med*. 2011;52:1400–1407.
29. Martin WR, Raichle ME. Cerebellar blood flow and metabolism in cerebral hemisphere infarction. *Ann Neurol*. 1983;14:168–176.
30. Ishikawa Y, Mukawa J, Kinjo T, et al. Crossed cerebellar diaschisis in putaminal hemorrhage: evaluation by the Xe-133 clearance method. *No To Shinkei (Tokyo)*. 1994;46:335–340.
31. Reinhard M, Muller T, Roth M, et al. Bilateral severe carotid artery stenosis or occlusion: cerebral autoregulation dynamics and collateral flow patterns. *Acta Neurochir (Wien)*. 2003;145:1053–1060.
32. Pappata S, Mazoyer B, Tran Dinh S, et al. Effects of capsular or thalamic stroke on metabolism in the cortex and cerebellum: a positron tomography study. *Stroke*. 1990;21:519–524.